

# Improving the photoelectrochemical activity of $\text{La}_5\text{Ti}_2\text{CuS}_5\text{O}_7$ for hydrogen evolution by particle transfer and doping†

Cite this: *Energy Environ. Sci.*, 2014, 7, 2239

Received 9th January 2014  
Accepted 18th March 2014

DOI: 10.1039/c4ee00091a

www.rsc.org/ees

Jingyuan Liu,<sup>a</sup> Takashi Hisatomi,<sup>a</sup> Guijun Ma,<sup>b</sup> Aki Iwanaga,<sup>a</sup> Tsutomu Minegishi,<sup>a</sup> Yosuke Moriya,<sup>a</sup> Masao Katayama,<sup>a</sup> Jun Kubota<sup>a</sup> and Kazunari Domen<sup>\*a</sup>

$\text{La}_5\text{Ti}_2\text{CuS}_5\text{O}_7$  doped with Sc in Ti sites generates photocathodic current at +0.88 V vs. RHE in photoelectrochemical water splitting and shows eight times higher photocurrent than undoped  $\text{La}_5\text{Ti}_2\text{CuS}_5\text{O}_7$ . The particle transfer method enabling good electrical contact and p-type doping increasing the majority carrier concentration contributes to the enhanced photoelectrochemical activity.

Photoelectrochemical (PEC) water splitting is an important technology for realizing artificial photosynthesis. Through photoexcitation of semiconductor electrodes by solar photons,  $\text{H}_2$  and  $\text{O}_2$  are produced from water at the surface of p-type and n-type semiconductor electrodes, respectively. Many semiconductors can generate a high photocurrent attributable to hydrogen or oxygen production when a sufficient external voltage is applied. However, it is likely that no single semiconductor electrodes can accomplish unassisted PEC water splitting at an appreciable rate under sunlight because of misalignment of the band edges with respect to the  $\text{H}_2$  and  $\text{O}_2$  evolution potentials or otherwise large band gap energies.<sup>1–6</sup>

A p/n-PEC cell based on two-step excitation of an electrically connected photocathode and photoanode has attracted much attention as a solution to the problem, because this system can generate sufficient photovoltage to drive the water splitting reaction and is potentially suitable for large-scale applications.<sup>7–12</sup> Although many p/n-PEC cells have been reported,<sup>13–16</sup> it is still a challenging task to develop a p/n-PEC cell that can realize the target solar-to-fuel conversion efficiency of 10% for practical artificial photosynthesis.<sup>17,18</sup> The efficiency of a p/n-PEC cell is greatly affected by the onset potentials of photocathodes and

## Broader context

A p/n-photoelectrochemical (PEC) cell based on two-step excitation has attracted much attention as a potential means for realizing artificial photosynthesis with the solar-to-fuel conversion efficiency reaching 10%. In order to archive high efficiency, a photocathode with positive onset potential for photocurrent is needed.  $\text{La}_5\text{Ti}_2\text{CuS}_5\text{O}_7$  is a semiconducting material applicable to PEC water splitting, although the characters and the potential of the material as photoelectrodes were not revealed sufficiently because of the lack of suitable fabrication methods of  $\text{La}_5\text{Ti}_2\text{CuS}_5\text{O}_7$  photoelectrodes. In this study, we used the particle transfer method to fabricate photoelectrodes of well-crystalline  $\text{La}_5\text{Ti}_2\text{CuS}_5\text{O}_7$  particles. The resultant  $\text{La}_5\text{Ti}_2\text{CuS}_5\text{O}_7$  photocathodes generated eight times higher photocathodic current than those with lower crystallinity prepared by pulsed laser deposition. The photocurrent of a  $\text{La}_5\text{Ti}_2\text{CuS}_5\text{O}_7$  photocathode was further boosted by p-type doping. Particularly, doping  $\text{La}_5\text{Ti}_2\text{CuS}_5\text{O}_7$  with 1% Sc in Ti sites resulted in the photocurrent onset potential of +0.88 V vs. RHE, which was one of the most positive potentials among ever-existing single p-type semiconductor photocathodes. The above remarkable properties revealed that particle transfer and p-type doping render  $\text{La}_5\text{Ti}_2\text{CuS}_5\text{O}_7$  one of the most promising photocathode materials for a p/n-PEC cell. Boosting the photocathodic current of  $\text{La}_5\text{Ti}_2\text{CuS}_5\text{O}_7$  further contributes to efficient solar hydrogen production.

photoanodes, because the maximum operation current density is determined by the intersection of the current–potential curves of the respective photoelectrodes.<sup>19–22</sup> Concerning photocathodes, as the onset potential of the photocathodic current becomes more positive, more efficient p/n-PEC cells can be fabricated. Thus, p-type semiconductor photocathodes with positive onset potentials need to be developed.

$\text{La}_5\text{Ti}_2\text{CuS}_5\text{O}_7$  is an oxysulphide p-type semiconductor that exhibits photocatalytic activity for both water reduction and oxidation under visible light irradiation in the presence of sacrificial reagents.<sup>23,24</sup> In addition,  $\text{La}_5\text{Ti}_2\text{CuS}_5\text{O}_7$  photoelectrodes prepared by pulsed laser deposition (PLD) and subsequent annealing under  $\text{H}_2\text{S}$  flow generated a photocathodic current. However, the photocathodic response was rather weak, presumably because of the low crystallinity of the  $\text{La}_5\text{Ti}_2\text{CuS}_5\text{O}_7$  thin film prepared by PLD. Refining the synthesis conditions revealed that  $\text{La}_5\text{Ti}_2\text{CuS}_5\text{O}_7$  with better crystallinity

<sup>a</sup>Department of Chemical System Engineering, School of Engineering, The University of Tokyo, 7-3-1 Hongo, Bunkyo-ku, 113-8656 Tokyo, Japan. E-mail: domen@chemsys.t.u-tokyo.ac.jp

<sup>b</sup>Department of Chemical System Engineering, School of Engineering, The University of Tokyo, 5-1-5 Kashiwanoha, Kashiwa-shi, 277-8589 Chiba, Japan

† Electronic supplementary information (ESI) available: Experimental details, characterization, PEC and photocatalytic activity of doped  $\text{La}_5\text{Ti}_2\text{CuS}_5\text{O}_7$ . See DOI: 10.1039/c4ee00091a



had higher photocatalytic activity.<sup>25</sup> It is natural to expect that  $\text{La}_5\text{Ti}_2\text{CuS}_5\text{O}_7$  with better crystallinity could exhibit higher PEC activity for water splitting as a photocathode. Unfortunately, methods to fabricate photoelectrodes of oxysulphide semiconductor particles had been lacking until very recently.

The particle transfer (PT) method can be used to fabricate photoelectrodes from semiconductor powders. A contact layer and a conductor layer of metals are deposited directly onto a photocatalyst particle layer to improve the electrical contact between the particles and metal layers.<sup>26,27</sup> For example, a photoanode of  $\text{LaTiO}_2\text{N}$  particles exhibited a photoanodic current 50 times higher than that obtained from a photoanode prepared on fluorine-doped tin oxide (FTO) by electrophoretic deposition at +1.23 V *vs.* reversible hydrogen electrode (RHE). This novel fabrication method can not only provide a good electrical contact at the interface between the conductive layer and photocatalyst particles, but also allow the application of highly crystalline semiconductor particles. In fact, PEC properties of copper gallium selenide electrodes fabricated by the PT method were studied recently.<sup>27</sup> Therefore, PT will enable investigation into the intrinsic PEC properties of high-crystallinity  $\text{La}_5\text{Ti}_2\text{CuS}_5\text{O}_7$  powder.

In this study, the performance of  $\text{La}_5\text{Ti}_2\text{CuS}_5\text{O}_7$  photoelectrodes fabricated by the PT method was assessed. Furthermore, doping with aliovalent cations was investigated as a way to improve the PEC activity. It was found that the addition of a small amount of sulphur during the synthesis of  $\text{La}_5\text{Ti}_2\text{CuS}_5\text{O}_7$  and the doping of Sc into Ti sites improved the photocathodic response significantly. The onset potential of the photocathodic current was +0.88 V *vs.* RHE, one of the most positive potentials ever obtained by a single p-type semiconductor photocathode, including CIGS and GaInP.<sup>28,29</sup>

$\text{La}_5\text{Ti}_2\text{CuS}_5\text{O}_7$  was prepared by a solid-state reaction. For metal-doped samples, the amount of  $\text{TiO}_2$  or  $\text{La}_2\text{O}_3$  was reduced, and the corresponding amounts of  $\text{Ta}_2\text{O}_5$ ,  $\text{Nb}_2\text{O}_5$ ,  $\text{Sc}_2\text{O}_3$ ,  $\text{Ga}_2\text{O}_3$ , or  $\text{CaO}$  were added.  $\text{La}_5\text{Ti}_2\text{CuS}_5\text{O}_7$  samples prepared in the presence of excess sulphur to avoid the generation of sulphur defects are designated  $\text{La}_5\text{Ti}_2\text{CuS}_5\text{O}_7(\text{S})$  in this work.  $\text{La}_5\text{Ti}_2\text{CuS}_5\text{O}_7$  photocathodes were fabricated by the PT method. A 2  $\mu\text{m}$  thick Au layer was deposited on the sample as a back contact layer by vacuum evaporation, and a 1 nm thick Pt layer was deposited as a catalyst by radio frequency magnetron sputtering unless otherwise noted. Photocurrent measurements were performed in a three-electrode configuration. A 0.1 M aqueous  $\text{Na}_2\text{SO}_4$  solution, whose pH was adjusted to 10 by NaOH, a Pt wire, and a Ag/AgCl electrode in a saturated KCl solution were used as electrolyte solution, counter electrode, and reference electrode, respectively. A 300 W Xe lamp was used as a light source. Photoelectrodes were irradiated through a cutoff filter ( $\lambda > 420$  nm). Other experimental details are provided in the ESI.<sup>†</sup>

Fig. 1 shows X-ray diffraction (XRD) patterns of representative  $\text{La}_5\text{Ti}_2\text{CuS}_5\text{O}_7$  powders. The sample prepared from a stoichiometric mixture of the precursors exhibited diffraction peaks attributable to  $\text{La}_5\text{Ti}_2\text{CuS}_5\text{O}_7$  and unknown impurities, as in a previous study.<sup>23</sup> The impurities are presumably mixed oxides of La–Ti–O. Upon the addition of excess sulphur into the precursor mixture, some of the impurity peaks disappeared.

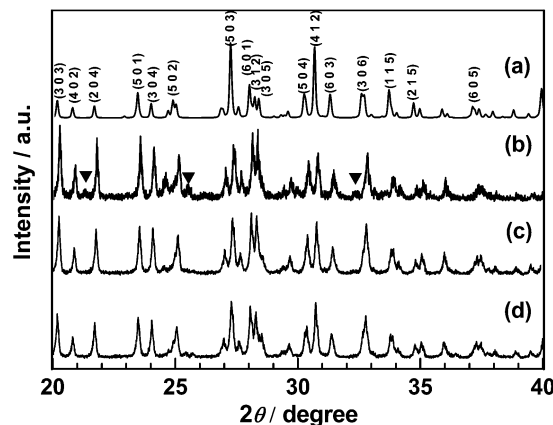


Fig. 1 XRD patterns for (a) the reference  $\text{La}_5\text{Ti}_2\text{CuS}_5\text{O}_7$  (ICSD #99612),<sup>23</sup> (b)  $\text{La}_5\text{Ti}_2\text{CuS}_5\text{O}_7$ , (c)  $\text{La}_5\text{Ti}_2\text{CuS}_5\text{O}_7(\text{S})$ , and (d) 1% Sc-doped  $\text{La}_5\text{Ti}_2\text{CuS}_5\text{O}_7(\text{S})$ . Triangles indicate impurity peaks weakened by adding excess sulphur.

Adding excess sulphur into the precursor increased the partial pressure of sulphur during the heat treatment. Similar approaches are taken for the synthesis of some oxides: tetravalent titanium ions could be reduced and oxygen vacancies were formed during the annealing synthesis of a titanium-based oxide semiconductor,<sup>30</sup> although this process could be suppressed by heating in an oxygen atmosphere.<sup>31</sup> The major diffraction peaks for all the  $\text{La}_5\text{Ti}_2\text{CuS}_5\text{O}_7(\text{S})$  doped with 1% Sc, Ga, Nb, Ta, and Ca (Fig. 1 and S1 in ESI<sup>†</sup>) were assigned to the  $\text{La}_5\text{Ti}_2\text{CuS}_5\text{O}_7$  phase. Scanning electron microscopy (SEM) images (Fig. S2 in ESI<sup>†</sup>) revealed that all the samples exhibited columnar particles and that doping with metal ions did not affect the particle morphologies significantly. UV-vis diffuse reflectance spectra (DRS) of the prepared samples (Fig. S3 in the ESI<sup>†</sup>) showed that the absorption edge of the doped samples were all close to 650 nm, which is comparable to that of undoped  $\text{La}_5\text{Ti}_2\text{CuS}_5\text{O}_7(\text{S})$ . These results indicate that the  $\text{La}_5\text{Ti}_2\text{CuS}_5\text{O}_7$  phase was obtained as the main product in the synthesis of the doped  $\text{La}_5\text{Ti}_2\text{CuS}_5\text{O}_7(\text{S})$ .

The current–potential (*I*–*E*) curves of  $\text{La}_5\text{Ti}_2\text{CuS}_5\text{O}_7$  photocathodes in aqueous solution under chopped illumination are plotted in Fig. 2. The onset potential of the photocurrent, *i.e.*, where the photocathodic current exceeded  $2 \mu\text{A cm}^{-2}$ , for the  $\text{La}_5\text{Ti}_2\text{CuS}_5\text{O}_7$  photocathode was +0.47 V *vs.* RHE, which was comparable to our previous work,<sup>24</sup> and the photocurrent at 0 V *vs.* RHE was improved by about an order of magnitude. This suggests that the  $\text{La}_5\text{Ti}_2\text{CuS}_5\text{O}_7$  photocathodes prepared by the PT method had a lower series resistance than those prepared by the previously reported PLD method. The onset potential for the photocathodic current in  $\text{La}_5\text{Ti}_2\text{CuS}_5\text{O}_7(\text{S})$  was +0.80 V *vs.* RHE, more positive by approximately 0.3 V, presumably because the formation of impurity phases was suppressed by the addition of excess sulphur into the precursor. The onset potential for the 1% Sc-doped  $\text{La}_5\text{Ti}_2\text{CuS}_5\text{O}_7(\text{S})$  photocathode was even more anodic: +0.88 V *vs.* RHE. In addition, the photocurrent density for the 1% Sc-doped  $\text{La}_5\text{Ti}_2\text{CuS}_5\text{O}_7(\text{S})$  photocathode was  $0.80 \text{ mA cm}^{-2}$  at 0 V *vs.* RHE, *i.e.*, roughly eight times higher than that for the undoped sample. Sc-doped  $\text{La}_5\text{Ti}_2\text{CuS}_5\text{O}_7(\text{S})$



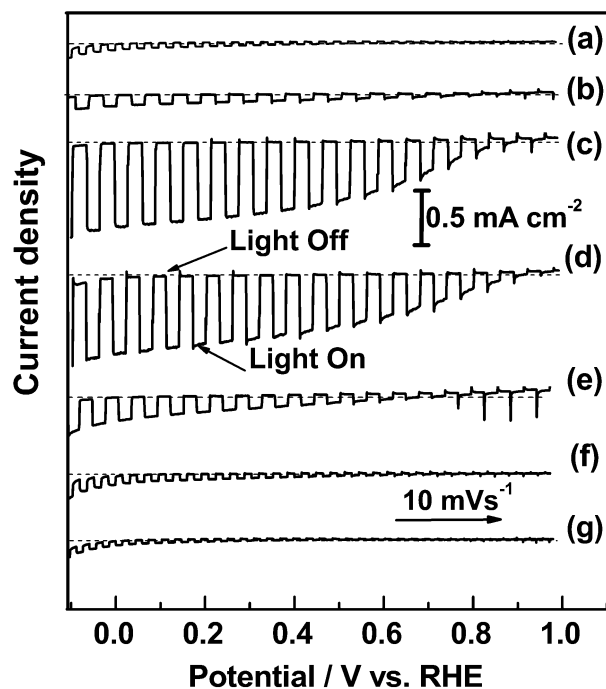


Fig. 2  $I$ - $E$  curves for (a)  $\text{La}_5\text{Ti}_2\text{CuS}_5\text{O}_7$  and (b) undoped, (c) 1% Sc-doped, (d) 1% Ga-doped, (e) 1% Ca-doped, (f) 1% Ta-doped, and (g) 1% Nb-doped  $\text{La}_5\text{Ti}_2\text{CuS}_5\text{O}_7(\text{S})$  photocathodes under chopped illumination. Pt was deposited by sputtering for  $\text{H}_2$  evolution. Electrolyte,  $\text{Na}_2\text{SO}_4$  aq (pH 10); light source, 300 W Xe lamp ( $\lambda > 420$  nm).

photocathodes modified with Ni instead of Pt also exhibited positive onset potential and the photocathodic current near the onset potential was comparable (Fig. S4 in the ESI†). This is encouraging in view of establishment of p/n-PEC cells, because the photocathodic current at the positive potential is a critical factor determining the overall efficiency. To determine the durability of  $\text{La}_5\text{Ti}_2\text{CuS}_5\text{O}_7$  photocathodes, the time course of the photocurrent was measured at 0 V vs. RHE (Fig. S5 in the ESI†). Sc-doped  $\text{La}_5\text{Ti}_2\text{CuS}_5\text{O}_7$  showed a photocurrent eight times higher than that for the undoped sample and maintained the photocathodic current for 2 h. The incident photon-to-current efficiency (IPCE) of the sample was 0.97% at 420 nm at 0 V vs. RHE and reached zero at 660 nm, as shown in Fig. S6 in the ESI†, which corresponded well to the absorption onset of the material. An enhanced PEC activity was also observed for  $\text{La}_5\text{Ti}_2\text{CuS}_5\text{O}_7(\text{S})$  doped with 1% Ga and 1% Ca (Fig. 2). In contrast, Ta- and Nb-doped  $\text{La}_5\text{Ti}_2\text{CuS}_5\text{O}_7(\text{S})$  showed lower PEC activity. These results suggest that an increase in the majority carrier concentration in  $\text{La}_5\text{Ti}_2\text{CuS}_5\text{O}_7$  by p-type doping, *i.e.*, doping with lower-valence cations, such as doping  $\text{Sc}^{3+}$  and  $\text{Ga}^{3+}$  into  $\text{Ti}^{4+}$  sites or doping  $\text{Ca}^{2+}$  into  $\text{La}^{3+}$  sites, improved the PEC activity. Various p-type dopants are currently being investigated to improve the PEC activity of  $\text{La}_5\text{Ti}_2\text{CuS}_5\text{O}_7$ .

One might suspect that doping of  $\text{Sc}^{3+}$  into  $\text{Ti}^{4+}$  would cause oxidation of  $\text{Cu}^+$  in  $\text{La}_5\text{Ti}_2\text{CuS}_5\text{O}_7$  to  $\text{Cu}^{2+}$  to maintain the charge balance of the material and deteriorate the semiconducting properties arising from  $\text{Cu}^+$ . Thus, changes in the valence states of  $\text{La}_5\text{Ti}_2\text{CuS}_5\text{O}_7$  doped at various levels of Sc were determined by Cu-K edge X-ray absorption near edge structure (XANES)

spectra. As shown in Fig. S7 in the ESI†, the X-ray absorption edge did not shift significantly with the Sc doping level, which suggested that the valence state of  $\text{Cu}^+$  was maintained in Sc-doped  $\text{La}_5\text{Ti}_2\text{CuS}_5\text{O}_7$ . Another concern would be the segregation of Sc species from the  $\text{La}_5\text{Ti}_2\text{CuS}_5\text{O}_7$  phase, that is, unsuccessful Sc doping. However, the XRD peaks clearly shifted toward smaller diffraction angles with increasing Sc doping level (Fig. 3), confirming that Sc was incorporated into the  $\text{La}_5\text{Ti}_2\text{CuS}_5\text{O}_7$  structure. The above findings suggest that the semiconducting properties of p-type  $\text{La}_5\text{Ti}_2\text{CuS}_5\text{O}_7$  were enhanced by doping it with Sc.

The PEC performance of  $\text{La}_5\text{Ti}_2\text{CuS}_5\text{O}_7(\text{S})$  photocathodes doped with Sc or Ga at different doping levels is listed in Table 1. The PEC activity of  $\text{La}_5\text{Ti}_2\text{CuS}_5\text{O}_7(\text{S})$  was improved by p-type doping. The photocurrent increased dramatically with increasing Sc doping level, reaching its maximum at 1%, and tended to decline gradually beyond 1%. Fig. 3 and Table 1 show that the full width at half maximum (FWHM) of the (501) and (304) diffraction peaks increased with increasing Sc doping level. Thus, the lower PEC performance at high doping levels may be due to the lower crystallinity of Sc-doped  $\text{La}_5\text{Ti}_2\text{CuS}_5\text{O}_7(\text{S})$ . In addition, the ionic radius of  $\text{Sc}^{3+}$  (88.5 pm) is 19% larger than that of  $\text{Ti}^{4+}$  in the six-coordination state. As the doping level of Sc into the Ti sites increased, so did the likelihood that part of the Sc species would be segregated. Nonstoichiometric cation compositions could enhance undesirable charge recombination and reduce the PEC activity of Sc-doped  $\text{La}_5\text{Ti}_2\text{CuS}_5\text{O}_7$ .

None of the doped  $\text{La}_5\text{Ti}_2\text{CuS}_5\text{O}_7$  exhibited a higher  $\text{H}_2$  evolution rate than the undoped sample in the photocatalytic  $\text{H}_2$  evolution reaction, unlike in the case of PEC  $\text{H}_2$  evolution (Fig. S8 in the ESI†). The opposite trend may be observed because an external voltage can be applied to the photocathodes so that photogenerated holes and electrons are forced to migrate to the back contact and the surface of the  $\text{La}_5\text{Ti}_2\text{CuS}_5\text{O}_7$  photoelectrodes, respectively, but not in the case of suspended  $\text{La}_5\text{Ti}_2\text{CuS}_5\text{O}_7$  particles. Additionally, in the photocatalytic reaction, both holes and electrons have to migrate to the surface. These factors would change the effects of element

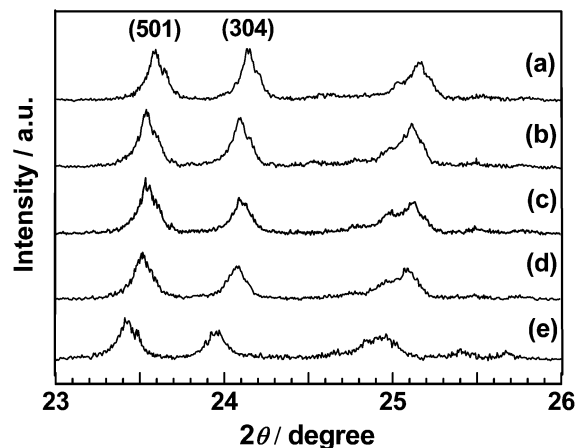


Fig. 3 XRD patterns for (a) undoped, (b) 1% Sc-doped, (c) 3% Sc-doped, (d) 5% Sc-doped, and (e) 10% Sc-doped  $\text{La}_5\text{Ti}_2\text{CuS}_5\text{O}_7(\text{S})$ .



**Table 1** Photoelectrochemical activity of doped  $\text{La}_5\text{Ti}_2\text{CuS}_5\text{O}_7(\text{S})$  photocathodes modified with Pt under visible light irradiation

Dopant	Doping rate/%	Onset potential/ V vs. RHE <sup>a</sup>	Photo-current at 0 V vs. RHE/ $\text{mA cm}^{-2}$	FWHM of (501) diffraction	FWHM of (304) diffraction
None	0	0.80	0.11	0.118	0.108
Sc	0.1	0.88	0.62	0.120	0.109
	1	0.89	0.80	0.133	0.115
	3	0.86	0.66	0.142	0.139
	5	0.86	0.52	0.154	0.145
	10	0.72	0.59	0.297	0.346
Ga	1	0.89	0.74	0.143	0.129
	3	0.83	0.44	0.150	0.154

<sup>a</sup> Potential at which photocurrent exceeded  $2 \mu\text{A cm}^{-2}$ .

substitution on the PEC and photocatalytic activity of  $\text{La}_5\text{Ti}_2\text{CuS}_5\text{O}_7$ .

## Conclusions

In conclusion,  $\text{La}_5\text{Ti}_2\text{CuS}_5\text{O}_7$  photocathodes fabricated by the PT method showed photocathodic currents ten times higher than those prepared by the PLD method at 0 V vs. RHE. The addition of sulphur to the precursor improved the photocathodic response because the formation of impurities was partly suppressed. p-Type doping further boosted the PEC activity of the  $\text{La}_5\text{Ti}_2\text{CuS}_5\text{O}_7$  photocathode because of an increase in the majority carrier concentration of  $\text{La}_5\text{Ti}_2\text{CuS}_5\text{O}_7$ . In particular, doping 1% Sc into Ti sites resulted in an eight-fold enhancement in the photocathodic current, while maintaining the stability. The  $\text{La}_5\text{Ti}_2\text{CuS}_5\text{O}_7$  photocathode is expected to be suitable for p/n-PEC cells because the onset potential of its photocathodic current is significantly more positive than those of other photocathodes, even without elaborate surface modification with n-type layers such as ZnO and CdS to form heterojunctions. Boosting the photocathodic current of  $\text{La}_5\text{Ti}_2\text{CuS}_5\text{O}_7$  further will contribute to the establishment of efficient p/n-PEC cells for solar water splitting.

## Acknowledgements

This work was supported by Grants-in-Aid for Specially Promoted Research (no. 23000009) and for Young Scientists (B) (no. 25810112) of the Japan Society for the Promotion of Science (JSPS), the Artificial Photosynthesis Project of the Ministry of Economy, Trade and Industry (METI) of Japan, and the Funding Program for World-Leading Innovative R&D on Science and Technology (FIRST Program) initiated by the Council for Science and Technology Policy (CSTP) of the Cabinet Office of Japan.

## Notes and references

- 1 E. Aharon-Shalom and A. Heller, *J. Electrochem. Soc.*, 1982, **129**, 2865.

- 2 N. Chandra, B. Wheeler and A. Bard, *J. Phys. Chem.*, 1985, **89**, 5037.
- 3 T. Bak, J. Nowotny, M. Rekas and C. Sorrell, *Int. J. Hydrogen Energy*, 2002, **27**, 991.
- 4 M. Gratzel, *Nature*, 2001, **414**, 338.
- 5 I. Cesar, A. Kay, J. Martinez and M. Gratzel, *J. Am. Chem. Soc.*, 2006, **128**, 4582.
- 6 M. Butler and D. Ginley, *J. Mater. Sci.*, 1980, **15**, 1.
- 7 A. Nozik, *Appl. Phys. Lett.*, 1976, **29**, 150.
- 8 E. Selli, G. Chiarello, E. Quartarone, P. Mustarelli, I. Rossetti and L. Forni, *Chem. Commun.*, 2007, 5022.
- 9 J. Bolton, *Sol. Energy*, 1996, **57**(1), 37.
- 10 S. Kocha, D. Montgomery, M. Peterson and J. Turner, *Sol. Energy Mater. Sol. Cells*, 1998, **52**, 389.
- 11 A. Nozik, *Appl. Phys. Lett.*, 1977, **30**, 567.
- 12 R. Kainthla, S. Khan and J. Bockris, *Int. J. Hydrogen Energy*, 1987, **12**, 381.
- 13 K. Ohashi, J. McCann and J. Bockris, *Nature*, 1977, **266**, 610.
- 14 K. Ohashi, J. McCann and J. Bockris, *Int. J. Hydrogen Energy*, 1977, **1**, 259.
- 15 J. Akikusa and S. Khan, *Int. J. Hydrogen Energy*, 2002, **27**, 863.
- 16 A. Fujishima and K. Honda, *Nature*, 1972, **238**, 37.
- 17 A. Bard and M. Fox, *Acc. Chem. Res.*, 1995, **28**, 141.
- 18 M. Weber and M. Kolodinski, *J. Electrochem. Soc.*, 1984, **131**, 1258.
- 19 M. Walter, E. Warren, J. Mckone, S. Boettcher, Q. Mi, E. Santori and N. Lewis, *Chem. Rev.*, 2010, **110**, 6446.
- 20 T. Hisatomi, F. Formal, M. Cornuz, J. Brillet, N. T  treault, K. Sivula and M. Gr  tzel, *Energy Environ. Sci.*, 2011, **4**, 2512.
- 21 D. Yokoyama, H. Hashiguchi, K. Maeda, T. Minegishi, T. Takata, R. Abe, J. Kubota and K. Domen, *Thin Solid Films*, 2011, **519**, 2087.
- 22 R. Abe, T. Takata, H. Sugihara and K. Domen, *Chem. Lett.*, 2005, **34**, 1162.
- 23 V. Meignen, L. Cario, A. Lafond, Y. Mo  lo, C. Guillot-Deudon and A. Meerschaut, *J. Solid State Chem.*, 2004, **177**, 2810.
- 24 M. Katayama, D. Yokoyama, Y. Maeda, Y. Ozaki, M. Tabata, Y. Matsumoto, A. Ishikawa, J. Kubota and K. Domen, *Mater. Sci. Eng., B*, 2010, **173**, 275.
- 25 T. Suzuki, T. Hisatomi, K. Teramura, Y. Shimodaira, H. Kobayashi and K. Domen, *Phys. Chem. Chem. Phys.*, 2012, **14**, 15475.
- 26 T. Minegishi, N. Nishimura, J. Kubota and K. Domen, *Chem. Sci.*, 2013, **4**, 1120.
- 27 H. Kumagai, T. Minegishi, Y. Moriya, J. Kubota, K. Domen, *J. Phys. Chem. C*, DOI: 10.1021/jp409921f.
- 28 R. C. Valderrama, P. J. Sebastian, J. Pantoja Enriquez and S. A. Gamboa, *Sol. Energy Mater. Sol. Cells*, 2005, **88**, 145.
- 29 H. Wang and J. A. Turner, *J. Electrochem. Soc.*, 2010, **157**, 173.
- 30 Q. Fu, F. Tietz and D. St  ver, *J. Electrochem. Soc.*, 2006, **153**(4), D74.
- 31 S. Havelia, K. Balasubramaniam, S. Spurgeon, F. Cormack and P. Salvador, *J. Cryst. Growth*, 2008, **310**, 1985.

